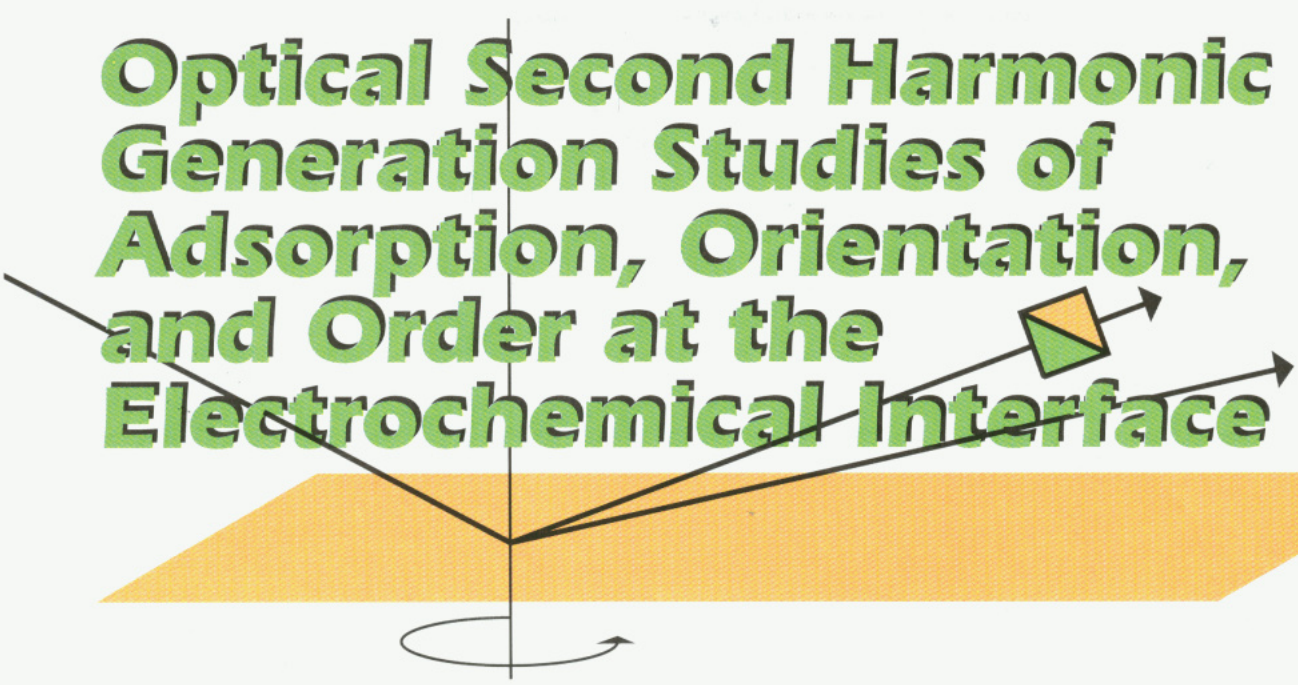# Optical Second Harmonic Generation Studies of Adsorption, Orientation, and Order at the Electrochemical Interface

Robert M. Corn
Department of Chemistry
University of Wisconsin—Madison
1101 University Ave.
Madison, WI 53706

The chemistry of solid–liquid interfaces affects a wide variety of important scientific and technological areas such as electroanalytical chemistry, heterogeneous catalysis, solar energy conversion, tribology, chemical sensors, and biological membranes. In each of these systems, a very small number of molecules at the surface can often control the macroscopic properties and direct the overall reactivity of the device or structure. For this reason,

INSTRUMENTATION

spectroscopists are interested in devising methods of monitoring the chemical and physical structures of such interfaces. A challenging problem for studies at condensed-phase interfaces is distinguishing between solution and interfacial species; this problem is particularly difficult for optical methods, given that the light employed in spectroscopic studies normally possesses a wavelength hundreds or thousands of times greater than typical interfacial distances.

Optical second harmonic generation (SHG) is an inherently surface-sensitive technique for studying the interface between two centrosymmetric media that overcomes this distance disparity (*1*). The second harmonic process (depicted in Figure 1) is the conversion of two photons of frequency ω to a single photon of frequency 2ω. In the electric dipole approximation, this process requires a noncentrosymmetric medium. For the interface between two centrosymmetric media, such as the interface between a face-centered cubic metal electrode and water, most of the second harmonic response is created within a nanometer of the metal surface. Higher order bulk contributions must also be considered in a rigorous analysis of the surface SHG response (*1*) but will not be discussed here.

With a demonstrated submonolayer sensitivity, a nearly instantaneous optical response time, and the ability to easily discriminate between surface species and species in the adjacent bulk media, SHG has been employed extensively at a wide variety of surfaces (air–solid [2], liquid–air [3], liquid–liquid [4], ultrahigh vacuum–single crystal [5–8], and electrochemical [9–17]). This article will focus on SHG measurements from platinum electrode surfaces; reviews of SHG studies at other electrochemical and nonelectrochemical surfaces can be found elsewhere (*1, 9*).

The second harmonic intensity $I(2\omega)$ from a platinum electrochemical surface is proportional to the square of its complex nonlinear susceptibility χ

$$I(2\omega) \propto |\mathbf{e}(2\omega) \cdot \chi \cdot \mathbf{e}(\omega)\mathbf{e}(\omega)|^2 I^2(\omega) \quad (1)$$

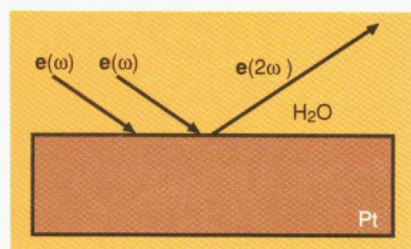where $I(\omega)$ is the input light power and $\mathbf{e}(\omega)$ and $\mathbf{e}(2\omega)$ are polarization vectors describing the input and output light fields, respectively (*1*). Because χ relates two input vectors to one output vector, it is a third-rank tensor and in general can have 18 distinct nonzero complex elements, χ_{ijk}. For most systems, the number of nonzero elements is greatly reduced by the surface symmetry. For example, if the surface is rotationally isotropic about the surface normal, as in the case of a polycrystalline platinum electrode, there are only three distinct nonzero tensor elements.

The experimental parameters used to measure the magnitudes of the tensor elements of a surface are shown in Figure 2. At a given wavelength, the SHG from a surface can be monitored as a function of input polarization, output polarization, incident angle, and (for anisotropic surfaces) azimuthal angle. For an electrochemical surface, changes in the SHG with changes in the electrode potential can be used to monitor the chemistry of the interface. A block diagram of the experimental apparatus employed in the SHG measurements is shown in Figure 3.

Pulses of light (typically 20 nJ energy, 2 ps pulse width, 4 MHz repetition rate) are focused onto a platinum electrode at a specific incident angle with a surface power density of $\sim$100 MW cm^{-2}. At this surface power density the SHG signal is quadratic with respect to the incident laser power (in accordance with Equation 1), and no surface damage is detected. The polarization of the incident fundamental beam is varied continuously from 0° (p-polarized, or parallel to the plane of incidence) to 90° (s-polarized, or perpendicular to the plane of incidence) by a $\lambda/2$ plate/polarizer combination. The reflected second harmonic light from the surface

Figure 1. Optical SHG at a platinum–water interface.

To first order, the conversion of light from frequency ω to frequency 2ω requires a noncentrosymmetric environment. Such an environment exists at the boundary of two centrosymmetric media, where the surface nonlinear susceptibility χ is the sole contributor to the second harmonic response.

$(2, 3, 14)$. For systems in which the SHG from the interface is dominated by the molecular contributions to the surface nonlinear susceptibility (χ_A), this orientation measurement is obtained through the analysis of the polarization dependence of the second harmonic response. The average molecular orientation at the surface is then estimated by assuming a molecular orientation distribution function and fitting the experimental data with this model.

The molecular second harmonic response of an adsorbed monolayer is normally enhanced by setting the wavelengths of the SHG process in resonance with a molecular electronic transition. Figure 4 depicts the three simplest possibilities for resonantly enhancing the molecular SHG signal. In Figure 4a, the fundamental wavelength is in resonance with a molecular electronic transition; in Figure 4b, the second harmonic wavelength is in resonance. Surface SHG experiments using this second enhancement mechanism have the advantage that the adsorbed monolayer is optically transparent at the fundamental wavelength, avoiding problems such as saturation or photobleaching of the molecules. Figure 4c shows the case where both the fundamental and the second harmonic wavelengths are in resonance with the molecular electronic transitions. The mo-
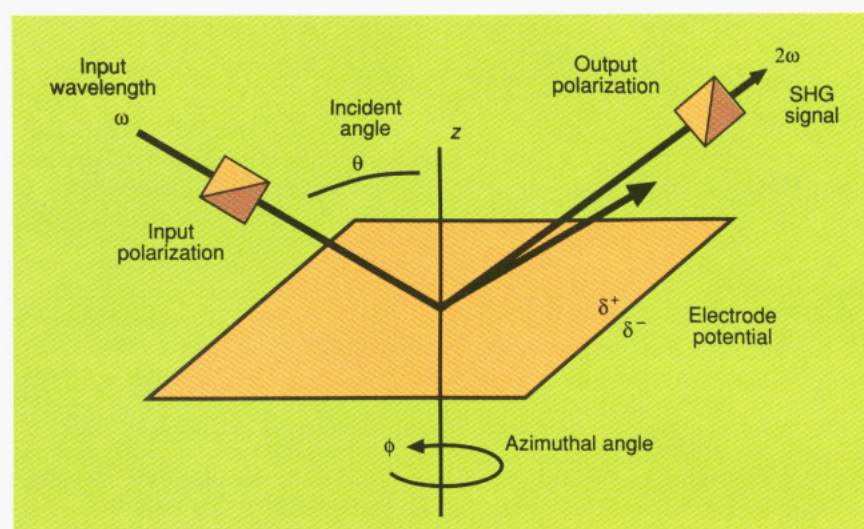
is collected and sent through a second polarizer set to pass either s-polarized or p-polarized light. Appropriate filters and a 0.175-m monochromator are used to reject any reflected fundamental light, and the SHG from the surface is detected with a cooled photomultiplier tube, the output of which is amplified and monitored with photon-counting electronics.

The nonlinear susceptibility of a surface can be described as the sum of three possible sources

$$\chi = \chi_S + \chi_A + \Delta\chi_I \qquad (2)$$

where χ_S is the nonlinear susceptibility of the platinum substrate, χ_A is the inherent nonlinear susceptibility of the molecules adsorbed onto the surface, and $\Delta\chi_I$ is the change in the nonlinear susceptibility of the platinum surface and adsorbate attributable to any surface–adsorbate interactions.

At a metal surface, χ_S is typically larger than χ_A. However, for platinum surfaces, changes in the nonlinear optical response upon adsorption ($\Delta\chi_I$) can be large enough to permit the detection of submonolayer quantities of an adsorbate. This indirect monitoring of chemisorption is called nonresonant SHG because the optical properties of the metal do not change rapidly with wavelength. In contrast to nonresonant SHG, with the proper selection of molecule, wavelength, and experimental geometry, χ_A can become the dominant contribution to χ. Experiments that use the inherent molecular nonlinear optical response are labeled resonant SHG in reference to the rapid variations of χ_A with wavelength.

Resonant SHG studies of molecular orientation

SHG has been employed extensively at both liquid and solid surfaces for the determination of average molecular orientation within an interfacial region

Figure 2. Experimental parameters for SHG measurements.

By monitoring the surface SHG signal as a function of input polarization, output polarization, incident angle, and azimuthal angle, the magnitudes of the various tensor elements of the nonlinear susceptibility χ can be measured.
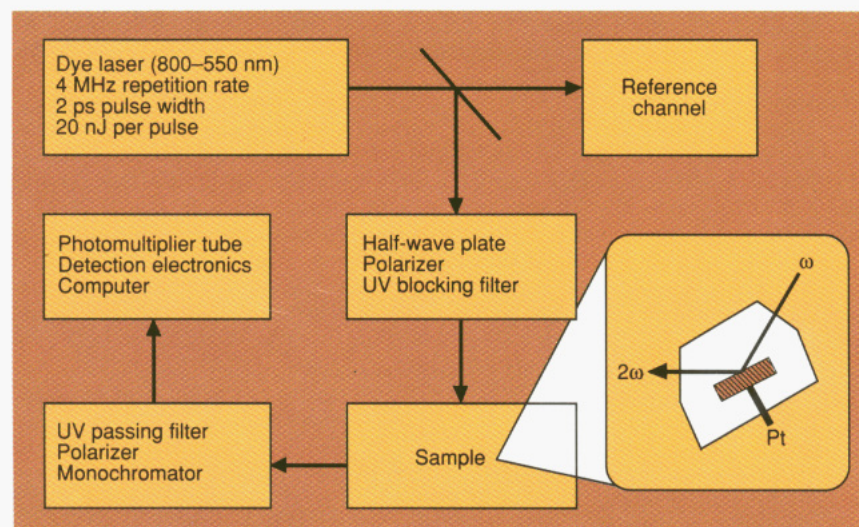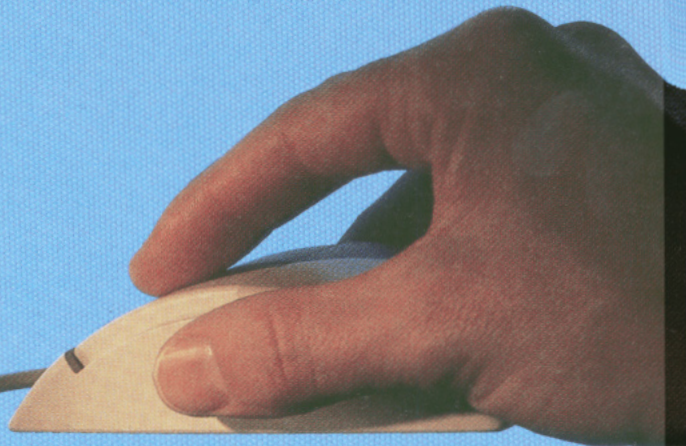

Figure 3. Block diagram of the experimental apparatus for SHG measurements.

The conversion efficiency for surface SHG is on the order of $10^{-10}\%$; however, this optical signal is easily detected with the photon-counting electronics.

Fast, easy
UV data
management ▶

User-guided
windowing ▶
environment

Multilevel ▶
macrolanguage

Here are a few pointers to cut your UV analysis time in half.

Introducing Perkin-Elmer's UV Data Manager (UVDM) Software. The easy way to improve your lab's performance. This powerful software package gives you total PC control of the Perkin-Elmer Lambda Series of UV/VIS spectrophotometers and accessories. UVDM allows rapid selection of operating conditions and collects, manipulates, and stores data. And prints your results in application-oriented formats.

UVDM is a simple-to-use windowing software featuring icons and drop-down menus. Just point and click for spectral

processing, quantitative analysis, data collection, and transfer procedures. Or double-click for on-line help.

UVDM features OBEY – the most advanced UV spectroscopy macrolanguage on the market. This BASIC-like programming language links together different functions. To automate time-consuming procedures, ensure reproducibility of a method, or develop specialized capabilities.

For more information on UVDM software, call 1-800-762-4000.

Or contact your local Perkin-Elmer Sales Office.
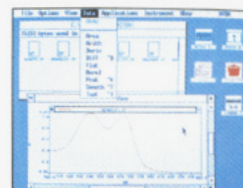
UVDM screen illustrating spectra data folder, spectral view window, and drop-down menu for data commands.

UV Data Manager is a powerful, yet easy to use software package compatible with Perkin-Elmer's Lambda Series UV/VIS Spectrophotometers and PC's utilizing 286 and 386SX microprocessors.

PERKIN ELMER

The Perkin-Elmer Corporation, Norwalk, CT 06859-0012

For Information Only Circle #111.   For a Sales Call Circle #112.

lecular SHG obtained in this configuration is called doubly resonant and provides the greatest enhancement of these three simplest resonant cases.

An example of a doubly resonant molecular system at an electrochemical surface for which an orientation measurement has been made is the adsorption of the dye molecule methylene blue onto a sulfur-modified platinum electrode (*14*). In this system, a monolayer of sulfur is chemisorbed onto the polycrystalline platinum surface prior to methylene blue adsorption. The sulfur monolayer serves two purposes: It enhances the chemisorption of the methylene blue cation, and it prevents any strong interactions of the dye molecule with the platinum surface.

The doubly resonant SHG at 292 nm from a monolayer of methylene blue at a polycrystalline platinum electrode as

Figure 5. Doubly resonant SHG from methylene blue at a sulfur-modified platinum electrode.

The potential dependence of the p-polarized SHG signal (solid line) at 292 nm and the current (dotted line) from a monolayer of methylene blue chemisorbed onto a sulfur-modified platinum electrode during the electrochemical reduction and reoxidation of the monolayer at a scan rate of 10 mV s^{-1}. The monolayer is chemisorbed onto the sulfur-modified platinum electrode in a phosphate buffer solution at pH 7.9. The SHG signal was obtained from a p-polarized fundamental 584-nm beam at an incident angle of 40.5°.

a function of potential, along with the cyclic voltammogram for the electrode, is shown in Figure 5. At a potential of −0.300 V versus SCE the chemisorbed dye molecule undergoes a two-electron reduction to leucomethylene blue; this electron transfer reaction shifts the electronic states of the adsorbed molecules and results in a loss of the SHG signal from the adsorbed monolayer. The low levels of the SHG signal after reduction of the dye molecule verify that the SHG from the interface can be

attributed almost entirely to the adsorbed methylene blue. A plot of the SHG signal from the surface at a fixed potential as a function of methylene blue surface coverage (Figure 6) also demonstrates how the nonlinear optical properties of the adsorbed dye molecules dominate the surface second harmonic response.

When the nonlinear optical response of the methylene blue molecule (*14*) and the experimentally determined macroscopic surface nonlinear susceptibility elements of χ are known, the molecular orientation distribution function for the adsorbed molecules can be determined. If it is assumed that there is no preferential molecular orientation with regard to the azimuthal angle ϕ about the surface normal, and that the aromatic rings of the adsorbed dye molecules are perpendicular to the surface, the average tilt angle $\langle \theta \rangle$ between the molecular symmetry axis and the surface normal can be estimated from the polarization dependence of the SHG signal.

Figure 6 depicts this experimentally determined molecular angle as a function of the surface coverage for the methylene blue adsorbed onto the sulfur-modified polycrystalline platinum electrode. As with all calculations, a number of assumptions enter into the determination of the average molecular orientation. For example, the dielectric constants for the monolayer must be estimated or measured to correctly ascertain the magnitudes of the tensor elements of χ, and from these tensor elements what is actually calculated is

Figure 4. Resonant enhancement mechanisms for molecular SHG.

The nonlinear second harmonic response of a molecule can be enhanced by tuning the wavelengths of the SHG process into resonance with a molecular electronic transition. The molecules can be in resonance with the fundamental laser wavelength (a), the second harmonic wavelength (b), or both (c). The last case is called doubly resonant SHG.
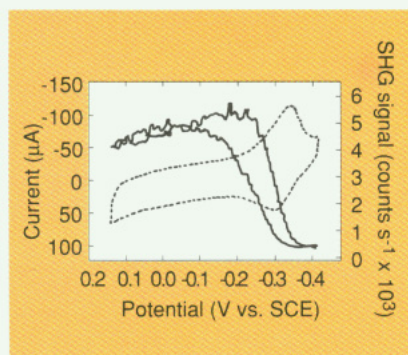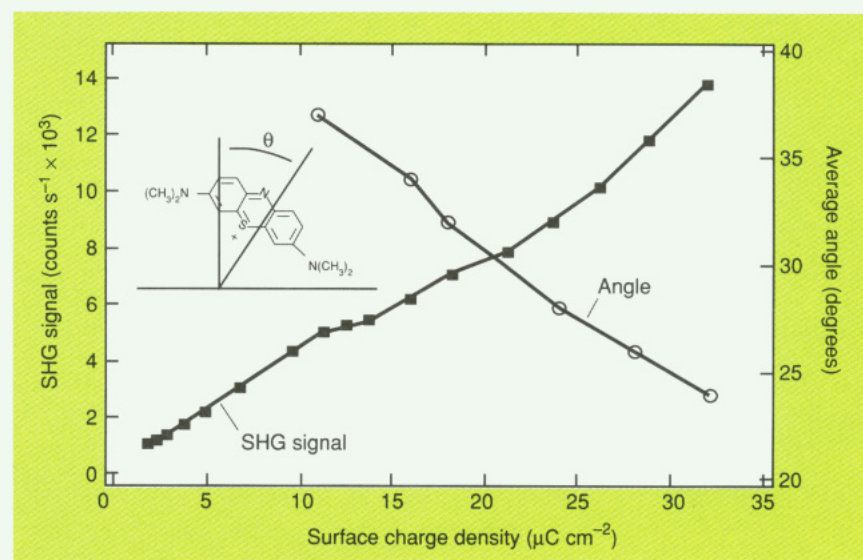

Figure 6. Molecular orientation calculation for methylene blue.

The p-polarized SHG signal (squares) and the calculated average molecular angle $\langle \theta \rangle$ (circles) from chemisorbed methylene blue at a sulfur-modified platinum electrode as a function of surface coverage, determined electrochemically from the surface charge density at a potential of +0.200 V versus SCE. A surface charge density of 32 μC cm^{-2} corresponds to a full monolayer of methylene blue. (Adapted from Reference 14.)

$\langle \cos^3 \theta \rangle / \langle \cos \theta \rangle$ instead of an angle $\langle \theta \rangle$. However, SHG measurements of the molecular orientation at several wavelengths can remove many of these ambiguities and assumptions, and the orientation calculation methodology used in the analysis of the surface SHG experiments is constantly being refined (18, 19). In addition to electrochemical interfaces, SHG is currently being applied to studies of molecular orientation in Langmuir–Blodgett films, at silica surfaces, and at liquid interfaces (1–4).

Nonresonant SHG studies of chemisorption

In the absence of any molecular transitions at the fundamental or second harmonic wavelengths, the second harmonic response from platinum electrodes is dominated by the nonlinear susceptibility of the surface metal atoms. On a variety of surfaces the changes in this nonresonant SHG ($\Delta \chi_I$ in Equation 2) have been used to indirectly monitor the chemisorption of species (5–7, 9, 11–13). For platinum surfaces the SHG signal was shown to provide a quantitative measure of the relative surface coverage of iodide, chloride, and bisulfate ions and other chemisorbed species (13).

The surface sensitivity and selectivity of the SHG signal enables one to measure surface chemisorption in the presence of a large amount of solution species and during solution reactions. However, in contrast to resonant SHG studies of molecules at electrode surfaces, use of the nonresonant SHG signal is a relatively nonspecific method that is only capable of monitoring the absorption of species that perturb the metal surface.

One chemisorbed species for which large changes are observed upon chemisorption is the monatomic hydrogen that exists on the platinum electrode prior to H_2 evolution. In Figure 7a the SHG signal at 302 nm from a polycrystalline platinum electrode in 0.1 M perchloric acid solution is plotted as a function of potential along with the cyclic voltammogram. Very large changes are observed in the hydrogen adsorption region; these changes can be quantitatively related to the amount of adsorbed hydrogen on the surface (13a). An increase in the SHG signal from a Pt(111) surface upon the chemisorption of hydrogen has also been observed in ultrahigh vacuum (7).

The presence of adsorbed hydrogen can also be monitored on single crystal platinum electrodes by changes in the nonresonant SHG signal from the surface. For Pt(111) electrodes, there has been much controversy concerning the

nature of the adsorbed hydrogen (20, 21). The SHG signal (p-polarized input and output) and cyclic voltammogram for a well-ordered Pt(111) surface produced by an iodine/CO treatment method (22) is shown in Figure 7b. A pronounced increase in the SHG signal is observed at potentials more negative than +0.480 V, the potential at which a broad anomalous wave is observed in the cyclic voltammogram. Clavilier et al. have attributed this voltammetric wave to the deposition of a strongly adsorbed hydrogen species (20), and Wagner and Ross have proposed that this hump in the cyclic voltammogram is a capacitive peak that results from the ordered adsorption of hydronium ions (21). For comparison, the potential dependence of the SHG signal and the cyclic voltammogram from a Pt(100) surface are shown in Figure 7c. On both this surface and the polycrystalline electrode (Figure 7a), an increase in the SHG is only observed during hydrogen deposition.
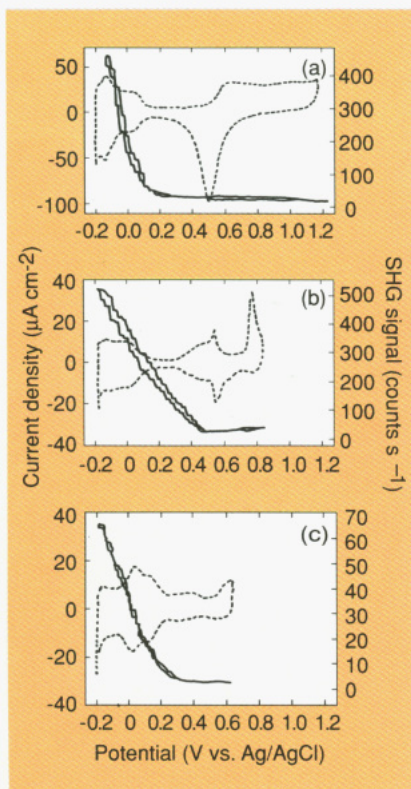
Figure 7. Nonresonant SHG studies of hydrogen adsorption at platinum electrodes.

The cyclic voltammogram (dotted line) and potential dependence (solid line) of the SHG signal at 302 nm (p-polarized input, p-polarized output) from: (a) a polycrystalline platinum surface, (b) a well-ordered Pt(111) surface, and (c) a well-ordered Pt(100) surface. On all three surfaces an increase in the nonresonant SHG signal is observed upon adsorption of monatomic hydrogen. The measurements were all obtained in 0.1 M perchloric acid at a scan rate of 20 mV s⁻¹.

On the basis of the above evidence, it is reasonable to relate the rise in the SHG signal on the Pt(111) surface to the presence of adsorbed hydrogen at all potentials more negative than +0.480 V on the well-ordered Pt(111) surface. However, one must remember that the nonresonant SHG signal is an indirect measurement of chemisorption and cannot definitively identify the chemisorbed species.

The chemisorption of the hydrogen in an adsorbed H_3O^+ species that strongly perturbs the platinum surface wave functions could also conceivably lead to the increase in the SHG signal. In fact, although the potential dependence of the SHG signal on all three platinum surfaces—Pt(111), Pt(100), and polycrystalline—is found to be very sensitive to the adsorption of hydrogen, the potential dependence of the SHG signal for the well-ordered Pt(111) surface in the double-layer region does not completely correlate with the cyclic voltammogram observed from the electrode.

A monotonic increase in the SHG signal is observed at all potentials more negative than +0.480 V. The lack of correlation of the SHG signal to the currents on this single crystal surface suggests that there are additional changes with potential in the electronic structure of the surface–hydrogen (or surface–hydronium ion) interaction.

SHG studies of ordered adsorption at single crystal surfaces

In addition to monitoring chemisorption, the nonresonant SHG signal can be used to identify the average surface symmetry at single crystal surfaces (1, 8, 10, 15–17). Because of the ordering of the single crystal surface, the second harmonic response is no longer rotationally isotropic about the surface normal. Additional tensor elements of χ will exist, depending on the average surface symmetry. These elements can be observed either by monitoring the variation of the second harmonic response as a function of azimuthal angle or by measuring the polarization dependence of the SHG signal at normal incidence (1, 17).

For example, the p-polarized SHG signal obtained from an s-polarized input beam, $I_{s,p}(2\omega)$, can be measured as a function of azimuthal angle, ϕ. For a Pt(111) surface, the symmetry of the first three surface layers is C_{3v}. (The symmetry of just the first monolayer is C_{6v}, but the SHG arises from all of the Pt atoms that are involved in the surface asymmetry.) For this surface, an additional nonzero tensor element χ_{xxx} is observed as compared with the isotropic surface and will lead to a rota-

tional anisotropy in the SHG signal.

The $I_{s,p}(2\omega)$ SHG signal at 302 nm from an iodine-coated Pt(111) electrode is plotted as a function of azimuthal angle in Figure 8a, where 0° corresponds to having the plane of incidence parallel to the x-axis (crystallographically the [2̄1̄1̄] axis) in Figure 8b. In Figure 8c the $I_{s,p}(2\omega)$ SHG signal is plotted in polar coordinates to highlight the threefold symmetry of the nonlinear optical response. The exact form of the $I_{s,p}$ anisotropy depends on the relative magnitudes and phases of the various surface tensor elements.
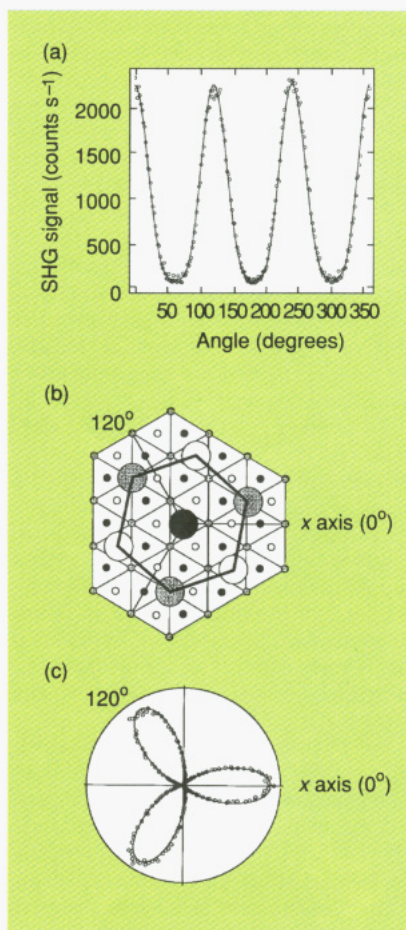
The presence of an adsorbate can

Figure 8. Rotational anisotropy measurements for an iodine-coated Pt(111) electrode.

(a) The $I_{s,p}(2\omega)$ (s-polarized input, p-polarized output) SHG signal as a function of azimuthal angle for a flame-annealed Pt(111) electrode with an adsorbed monolayer of atomic iodine in 0.1 M $HClO_4$ at an electrode potential of +0.200 V. (Adapted from Reference 15a.) (b) Diagram of the first three monolayers of a Pt(111) surface with a ($\sqrt{7} \times \sqrt{7}$)R19.1° adsorbed iodine monolayer (see text). Larger circles represent iodine atoms; smaller circles represent platinum atoms. Shading indicates height of each atom; black represents the top surface layer, and gray and white represent the second and third surface layers, respectively. (c) Polar plot of the $I_{s,p}(2\omega)$ SHG signal highlighting the threefold symmetry of the second harmonic response.

ONCE YOU'VE SEEN OUR MOISTURE ANALYSIS SYSTEM, YOU MAY SEE OTHER SYSTEMS A LITTLE DIFFERENTLY.

Now, there's a better way to do moisture analysis. The AQUASTAR® C-2000 Coulometric Titration System.

It can detect as little as 10 μg of water, and titrate 1 mg with ±0.3% accuracy in less than a minute. With the touch of a button, it titrates your sample, determines the end point, and gives you the answer in ppm or weight percent. You can also do statistical analysis, plot volume vs. time curves, and transfer the data to a personal computer.

Even if you already have a titrator, our KF reagents can help you get better results. The AQUASTAR Coulomat Single Solution is up to 50% faster than conventional KF reagents, has twice the absorption capacity, and gives you better accuracy—on *any* brand of coulometric KF titrator. And since it's pyridine and chloroform free, you never have to handle carcinogens.

So if you're searching for dependable moisture analysis, come right to the source. Call **1-800-222-0342** and ask to see a demonstration of our AQUASTAR KF Titrators and Reagents.

EM ®

EM SCIENCE
Quality is good chemistry.

A Division of EM Industries, Inc., P.O. Box 70, 480 Democrat Rd., Gibbstown, NJ 08027, Associate of E. Merck, Darmstadt, Germany

CIRCLE 32 ON READER SERVICE CARD

both modify the magnitude and phase of an existing surface tensor element and create new ones. If the adsorbate reduces the average surface symmetry, additional nonzero elements of χ will appear in the rotational anisotropy. For example, iodine is known to adsorb onto the Pt(111) surface in a $\sqrt{7} \times \sqrt{7}$ overlayer structure (23) shown in Figure 8b. The iodine atoms form a C_{3v} monolayer with a symmetry axis that is rotated by 19.1° from the substrate crystal symmetry axis. This reduces the combined symmetry of the substrate and monolayer from C_{3v} to C_3, and leads to the possibility of nonzero χ_{xyz} and χ_{yyy} tensor elements for the surface.

Figure 9a shows the $I_{p,s}(2\omega)$ SHG signal at 302 nm for the Pt(111)–iodine monolayer system that was obtained with p-polarized input light and s-polarized output light (as compared with the $I_{s,p}(2\omega)$ data shown in Figure 8, which used s-polarized input light and p-polarized output light). This SHG anisotropy can be interpreted in terms of the existence of a nonzero χ_{xyz} element. The $\sqrt{7} \times \sqrt{7}$ iodine monolayer reduces the surface symmetry and leads to the threefold pattern shown in Figure 9a. If only the χ_{xxx} element contributed to the rotational anisotropy, the SHG signal would be a sixfold symmetric pattern. Upon removal of the iodine by CO displacement and subsequent oxidation, the sixfold pattern expected from a C_{3v} substrate is observed (Figure 9b).

Figure 9c shows the $I_{p,s}(2\omega)$ anisotropy observed for the Pt(111) surface in the potential region of hydrogen adsorption; the pattern indicates that the adsorbed hydrogen also alters the sixfold symmetry of the SHG response. Note that in this particular choice of input and output polarizations, no isotropic contributions to the SHG signal occur; only terms indicating ordered adsorption contribute to the surface second harmonic response.

A final caveat that must be mentioned is that in all of the anisotropy experiments the SHG signal measures the average surface symmetry (much like the average molecular orientation). In other words, a surface that has equal amounts of two possible C_3 domains would have an average surface symmetry of C_{3v}, not C_3. In the experiments on platinum single crystal electrodes an unequal domain distribution for the overlayers permits the determination of the average surface symmetry from the SHG measurements (15). SHG anisotropy measurements are sensitive not only to surface symmetry changes upon chemisorption, but also to symmetry changes resulting from surface reconstruction. In addition to platinum, SHG rotational anisotropy measurements currently are being made on silver and gold single crystal electrodes (9, 10, 16, 17).

Future extensions

As laser technology continues to improve, the quality and number of SHG experiments at electrode surfaces will undoubtedly increase and branch out in several directions. For resonant molecular SHG studies, experiments at transparent electrodes instead of metal surfaces should lead to orientation measurements from a wider variety of mol-
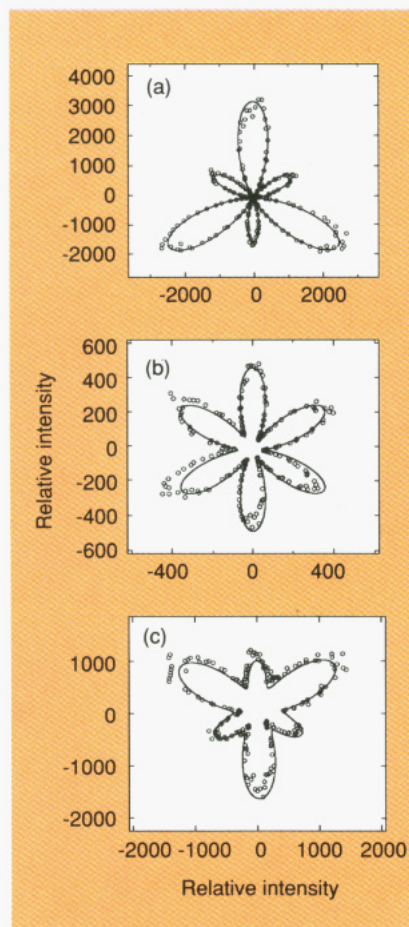
Figure 9. Changes in the SHG rotational symmetry plots for a Pt(111) electrode upon chemisorption.

Polar plots of the $I_{p,s}(2\omega)$ (p-polarized input, s-polarized output) SHG signal for a flame-annealed Pt(111) electrode (a) with an adsorbed monolayer of atomic iodine in 0.1 M HClO$_4$ at an electrode potential of +0.200 V, (b) at an electrode potential of +0.200 V after the removal of the iodine monolayer, and (c) at a potential of −0.175 V in the hydrogen adsorption region. A surface with C_{3v} symmetry will yield a symmetric sixfold pattern; the presence of a monolayer of iodine or hydrogen reduces the combined surface symmetry and results in a threefold symmetry for the SHG signal. The polar plots are labeled with the relative intensities of the SHG signal from the three surfaces along the x and y crystal axes.

ecules. For nonresonant SHG studies, a better theoretical understanding of the surface second harmonic response and more experimental correlations with ultrahigh vacuum data will enhance the interpretation of the changes in the SHG signal upon chemisorption.
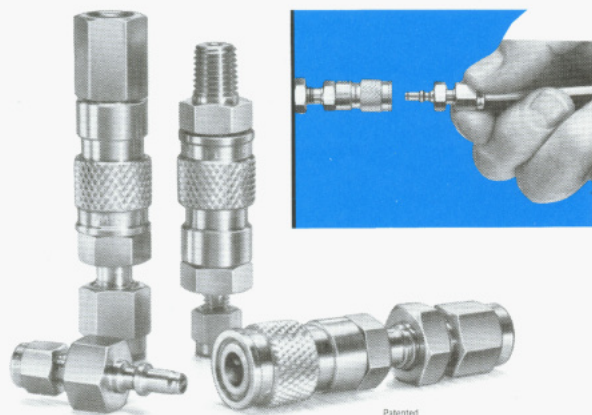
At single crystal electrodes, further studies of average surface symmetry at a variety of electrode surfaces should be possible; two-beam measurements will permit the more accurate determination of the various elements of χ. Another use of two-beam measurements will be the implementation of picosecond time-resolved SHG measurements of reactions at electrochemical interfaces. Such experiments have been performed at liquid–air interfaces (24).

SHG is the simplest of a variety of nonlinear optical experiments that can be performed at surfaces. In particular, the use of sum generation will extend the wavelength region over which molecular resonances can be observed, and the possibility of probing vibrational resonances with IR–vis sum generation experiments (25) is just beginning. Both techniques possess the same surface sensitivity that is inherent in all of the SHG measurements.

References

(1) a. Shen, Y. R. *The Principles of Nonlinear Optics;* Wiley: New York, 1984; b. Shen, Y. R. *Annu. Rev. Phys. Chem.* **1989,** *40,* 327.
(2) a. Heinz, T. F.; Chen, C. K.; Ricard, D.; Shen, Y. R. *Phys. Rev. Lett.* **1982,** *48,* 478; b. DiLazzaro, P.; Mataloni, P.; DeMartini, F. *Chem. Phys. Lett.* **1985,** *114,* 103; c. Dick, B.; Gierulski, A.; Marowsky, G.; Reider, G. A. *Appl. Phys.* **1985,** *B38,* 107; d. Mazely, T. L.; Hetherington III, W. M. *J. Chem. Phys.* **1987,** *87,* 1442; e. Cresswell, S. A.; Steehler, J. K. *Appl. Spectrosc.* **1987,** *41,* 1329.
(3) a. Hicks, J. M.; Kemnitz, K.; Eisenthal, K. B.; Heinz, T. F. *J. Phys. Chem.* **1986,** *90,* 560; b. Kemnitz, K.; Bhattacharyya, K.; Hicks, J. M.; Pinto, G. R.; Eisenthal, K. B.; Heinz, T. F. *Chem. Phys. Lett.* **1986,** *131,* 285.
(4) Grubb, S. G.; Kim, M. W.; Rasing, T.; Shen, Y. R. *Langmuir* **1988,** *4,* 452.
(5) Tom, H.W.K.; Mate, C. M.; Zhu, X. D.; Crowell, J. E.; Heinz, T. F.; Somorjai, G. A.; Shen, Y. R. *Phys. Rev. Lett.* **1984,** *52,* 348.
(6) a. Heskett, D.; Song K. J.; Burns, A.; Plummer, E. W.; Dai, H. L. *J. Chem. Phys.* **1986,** *85,* 7490; b. Heskett, D.; Urbach, L. E.; Song, K. J.; Plummer, E. W.; Dai, H. L. *Surf. Sci.* **1988,** *197,* 225; c.

Song, K. J.; Heskett, D.; Dai, H. L.; Liebsch, A.; Plummer, E. W. *Phys. Rev. Lett.* **1988,** *61,* 1380.
(7) Grubb, S. G.; DeSantolo, A. M.; Hall, R. B. *J. Phys. Chem.* **1988,** *92,* 1419.
(8) a. Driscoll, T. A.; Guidotti, D. *Phys. Rev.* **1983,** *B28,* 1171; b. Tom, H.W.K.; Heinz, T. F.; Shen, Y. R. *Phys. Rev. Lett.* **1983,** *51,* 1983; e. Heinz, T. F.; Loy, M.M.T.; Thompson, W. A. *Phys. Rev. Lett.* **1985,** *54,* 63; d. Tom, H.W.K.; Aumiller, G. D. *Phys. Rev.* **1986,** *B33,* 8818; e. Hamilton, J. C.; Williams, L. R.; Anderson, R.J.M. *Chem. Phys. Lett.* **1990,** *167,* 507.
(9) a. Richmond, G. L.; Robinson, J. M.; Shannon, V. L. *Prog. Surf. Sci.* **1988,** *28,* 1; b. Richmond, G. L. *Langmuir* **1986,** *2,* 132.
(10) a. Shannon, V. L.; Koos, D. A.; Kellar, S. A.; Huiang, P.; Richmond, G. L. *J. Phys. Chem.* **1989,** *93,* 6434; b. Shannon, V. L.; Koos, D. A.; Richmond, G. L. *J. Phys. Chem.* **1987,** *91,* 5548.
(11) a. Corn, R. M.; Romagnoli, M.; Levenson, M. D.; Philpott, M. R. *J. Phys. Chem.* **1984,** *81,* 4127; b. Corn, R. M.; Romagnoli, M.; Levenson, M. D.; Philpott, M. R. *Chem. Phys. Lett.* **1984,** *106,* 30.
(12) Campbell, D. J.; Corn, R. M. *J. Phys. Chem.* **1987,** *91,* 5668.
(13) a. Campbell, D. J.; Corn, R. M. *J. Phys. Chem.* **1988,** *92,* 5796; b. Campbell, D. J.; Lynch, M. L.; Corn, R. M. *Langmuir,* in press.
(14) Campbell, D. J.; Higgins, D. A.; Corn, R. M. *J. Phys. Chem.* **1990,** *94,* 3681.
(15) a. Lynch, M. L.; Corn, R. M. *J. Phys. Chem.* **1990,** *94,* 4382; b. Lynch, M. L.;

Barner, B. J.; Corn, R. M. *J. Electroanal. Chem.*, in press.

(16) Friedrich, A.; Pettinger, B.; Kolb, D. M.; Lupke, G.; Steinhoff R.; Marowsky, G. *Chem. Phys. Lett.* **1989,** *163,* 123.

(17) Miragliotta, J.; Furtak, T. E. *Phys. Rev.* **1988,** *B37,* 1028.

(18) Guyot-Sionnest, P.; Shen, Y. R.; Heinz, T. F. *Appl. Phys.* **1987,** *B42,* 237.

(19) Peterson, E. S.; Harris, C. B. *J. Chem. Phys.* **1989,** *91,* 2683.

(20) a. Clavilier, J.; Faure, R.; Guinet, G.; Durand, R. *J. Electroanal. Chem.* **1980,** *107,* 205; b. Clavilier, J. *J. Electroanal. Chem.* **1980,** *107,* 211.

(21) a. Wagner, F. T.; Ross, P. N. *J. Electroanal. Chem.* **1983,** *150,* 141; b. Ross, P. N. *Electrochemical Surface Science, Molecular Phenomenon at Electrode Surfaces;* ACS Symposium Series 378; American Chemical Society: Washington, DC, 1988; Chapter 3.

(22) a. Zurawski, D.; Rice, L.; Hourani, M.; Wieckowski, A. *J. Electroanal. Chem.* **1987,** *230,* 221; b. Wieckowski, A.; Schardt, B. C.; Rosasco, S. D.; Stickney, J. L.; Hubbard, A. *Surf. Sci.* **1984,** *146,* 115.

(23) a. Felter, T. E.; Hubbard, A. T. *J. Electroanal. Chem.* **1979,** *100,* 473; b. Schardt, B. C.; Yau, S.; Rinaldi, F. *Science* **1989,** *243,* 1050.

(24) Sitzmann, E. V.; Eisenthal, K. B. *J. Phys. Chem.* **1988,** *92,* 4579.

(25) a. Shen, Y. R. *Nature* **1989,** *337,* 519; b. Harris, A. L.; Chidsey, C.E.D.; Levinos, N. J.; Loiacono, D. N. *Chem. Phys. Lett.* **1987,** *141,* 350.

Robert M. Corn received his B.A. degree in chemistry summa cum laude from the University of California—San Diego in 1978 and his Ph.D. in chemistry from the University of California, Berkeley, in 1983. He joined the faculty of the University of Wisconsin—Madison, where he is currently an assistant professor, after a postdoctoral fellowship at the IBM Research Laboratories in San Jose, CA, and a one-year visiting assistant professorship at Swarthmore College in Swarthmore, PA. His research interests include nonlinear optical spectroscopy at surfaces, FT-IR and Raman spectroscopy of thin films and interfaces, and the theory of dephasing and motional effects in the IR spectra of crystalline solids.